GASTROINTESTINAL

CrossMark

A New Model for MR Evaluation of Liver Function with Gadoxetic Acid, Including Both Uptake and Excretion

Daniel Truhn[1] · Christiane K. Kuhl[1] · Alexander Ciritsis[1] · Alexandra Barabasch[1] · Nils A. Kraemer[1]

Abstract

Objectives Most existing models that are in use to model hepatic function through assessment of hepatic gadoxetic acid enhancement kinetics do not consider quantitative measures of gadoxetic excretion. We developed a model that allows a simultaneous quantitation of uptake and excretion of liver specific contrast agents. The aim was to improve the assessment of hepatic synthetic function, and provide quantitative measures of hepatic excretion function.

Methods Sixteen patients underwent dynamic T1-weighted turbo gradient echo imaging at 1.5 T prior and after bolus injection of gadoxetic acid at 0.1 ml/kg. DCE-images were obtained for 30 min after injection. A dual-inlet two-compartment model was then used to fit the measured liver signal values. Four tissue parameters (extracellular volume fraction, arterial flow fraction, uptake rate and excretion half-time) were extracted for each liver segment.

Results The proposed model provided a good fit to acquired data. Mean values for arterial flow fraction (0.08+-0.04), extracellular volume (0.20±0.08) and uptake rate (4.02 ±1.32 /100 ml/min) were comparable to those obtained with the conventional model (0.08±0.05, 0.21±0.12, and 4.93±1.74), but exhibited significantly less variation and improved fit quality.

Conclusions The proposed model is more accurate than existing conventional models and provides an additional excretion parameter.

Key Points
• *Models of hepatic contrast agent uptake can be extended to include excretion.*
• *Including an additional excretion parameter improves accuracy of the model.*
• *Standard diagnostic sequences can be extended to incorporate the model.*

Keywords Hepatobiliary elimination · Magnetic resonance imaging · Contrast media · Patient-specific modelling

Abbreviations and acronyms
DCE   Dynamic contrast-enhanced
MRI   Magnetic resonance imaging
ROI   Region of interest

Introduction

Dynamic contras- enhanced (DCE) magnetic resonance (MR) imaging (MRI) of the liver has become a standard diagnostic tool to detect, grade and classify diffuse as well as focal liver disease. The introduction of hepatobiliary contrast agents such as gadoxetic acid has further enhanced diagnostic accuracy and helps identify and classify a variety of liver lesions.

An emerging application of gadoxetic acid-enhanced liver MRI is to assess liver function. Several studies demonstrated that a quantitative measure of hepatic contrast uptake can be used for this purpose, because gadoxetic acid is taken up by hepatocytes mediated by the organic anion transporting polypeptide [1]. In animal models, an inverse relationship between experimentally-induced hepatic dysfunction and hepatic uptake of gadoxetic acid has been established [2, 3]. Moreover, the reduced hepatic uptake of gadoxetic acid has been linked to down-regulated membrane transport proteins in damaged liver tissue [4]. Gadoxetic-enhanced imaging has thus been proposed to rate the degree of steatohepatitis [5], liver cirrhosis [6–8] or liver function [9, 10]. Most published models that are in use to assess liver function are based on measures of

✉ Daniel Truhn

[1] Department of Diagnostic and Interventional Radiology, RWTH University Hospital Aachen, Pauwelsstraße 30, 52074 Aachen, Germany

🌀 Springer

hepatic gadoxetic acid enhancement, i.e. consider hepatic uptake only. However, hepatic uptake of gadoxetic acid will always be accompanied by gadoxetic acid excretion. Both processes occur more or less simultaneously, and will mutually influence the net intracellular gadolinium amount, and, thus, the resulting hepatic signal intensity. Accordingly, for a precise assessment of liver function, both processes need to be observed and considered. A recently published study demonstrated the feasibility of extracting hepatic excretion and uptake in a study of ten volunteers [11]; however, it lacks the comparison to models that consider uptake only.

Moreover, there is increasing evidence that hepatic excretion per se is a parameter that provides diagnostically useful information on liver function. However, published clinical studies that investigate the utitility of gadoxetic acid excretion used qualitative or semi-quantitative metrics, e.g. measured the time it takes until bile ducts are opacified [12–14].

We hypothesised that a model that accounts for both hepatic uptake as well as hepatic excretion should improve the assessment of quantitative functional information inherent to hepatic gadoxetic acid enhancement kinetics as compared to existing models considering uptake only.

Materials and methods

Tissue model

A dual-inlet two-compartment model (Fig. 1) was considered to describe the uptake into and the excretion out of the
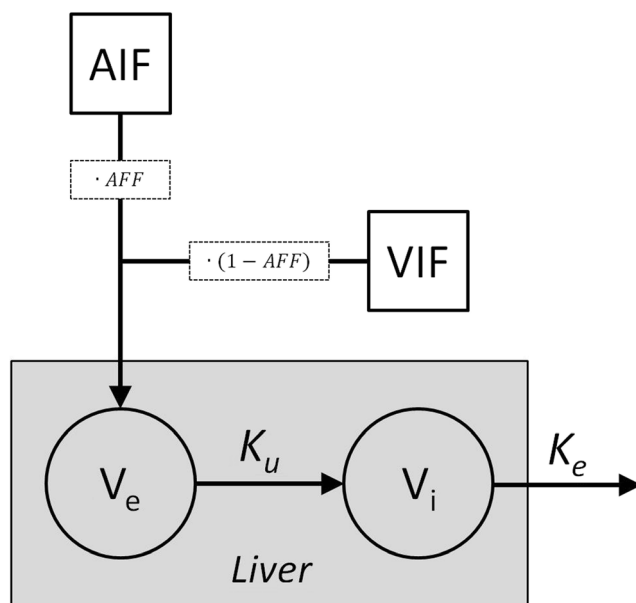

Fig. 1 Schematic diagram of the dual-inlet two-compartment uptake and excretion model. *AFF* arterial flow fraction, *AIF* arterial input flow, *VIF* portal venous input flow, *Ve* extracellular volume fraction, *Vi* intracellular volume fraction, *Ku* uptake rate, *Ke* excretion rate

intracellular space. The model is defined by four tissue parameters: (1) The arterial flow fraction AFF defined as $(F_a)/(F_a+F_p)$, where F_a and F_p are the arterial and portal venous flow respectively. (2) The intracellular volume fraction V_i in ml per 100 ml of liver tissue. (3) The intracellular uptake rate K_u, defined as in [15]. (4) The excretion rate K_e out of the intracellular space, defined analogously to K_u. The model assumes that gadoxetic acid is well mixed in the extracellular space and that the arterial and portal venous delay times are negligible on the timescale of the measurements. The extracellular concentration can therefore be described as [16]:

$$C_e = AFF \cdot C_a + (1-AFF) \cdot C_p$$

Here C_e, C_a and C_p represent the extracellular, arterial and portal venous contrast agent concentrations, respectively.

The differential equation described previously [15] was appended by a term K_eC_i, which accounts for excretion into the bile duct:

$$V_i \frac{dC_i}{dt} = K_uC_e - K_eC_i$$

C_i represents the concentration of contrast agent in the intracellular compartment and K_u and K_e are the rate constants for the uptake and excretion, respectively.

The solution to this inhomogeneous differential equation is given by:

$$C_i(t) = \frac{1}{V_i} \int_0^t K_u C_e(\tau) \cdot \exp\left(-\frac{K_e}{V_i} \cdot (t-\tau)\right) d\tau.$$

With knowledge of both C_e and C_i, the mean hepatic tissue concentration C_L can finally be calculated as:

$$C_L = (1-V_i)C_e + V_iC_i$$

where the extracellular volume fraction V_e is expressed as $(1-V_i)$.

To get a more intuitive grasp of the extracted parameters, the effective excretion half-time was defined as:

$$T_{\frac{1}{2},e} = \frac{\ln(2)}{\left(\frac{K_e}{V_i}\right)}.$$

This can be understood as the time it takes to eliminate half of the intracellular gadoxetic acid if uptake was stopped, i.e. if the blood concentration of gadoxetic acid was zero.

Patients

After approval by the ethics committee (EK 036/13) and after obtaining written informed consent, 16 patients (six female, ten male) who underwent hepatic gadoxetic-enhanced MRI for clinical indications were included in this feasibility study.

Two patients were excluded due to the presence of severe breathing motion-related artefacts, which prohibited a reliable determination of the signal intensity in the portal vein, leaving n=14 patients for the subsequent analysis. The patients' mean age was 59 years (range: 41–73). Patients were referred for liver MRI in order to rule out hepatic metastases. In all cases, there were no signs for focal or parenchymal liver disease. Due to their underlying disease, all but one patient had received prior chemotherapy. There were no clinical or radiological signs of chemotherapy-associated liver damage [17]. All patients belonged to class A in the Child-Pugh classification system. To exclude hepatic steatosis due to chemotherapy, Dixon's two-point method was employed to determine hepatic fat fraction as described in [18].

Data acquisition

The MRI examinations were performed on a clinical 1.5 T scanner (Achieva, Philips Healthcare, Hamburg, Germany) using a 16-channel torso receiver coil (Sense XL Torso Coil, Philips Healthcare).

During acquisition of the DCE MR data, 0.1 ml/kg of gadoxetic acid (Primovist: Bayer) was injected into the right or left anterior cubital vein at a rate of 2 ml/s and flushed with 20 ml of saline at the same rate. The DCE MR series comprised a T1-weighted gradient echo sequence used in clinical routine; the imaging parameters were as follows: three dimensional T1-weighted spoiled gradient echo sequences with 8-mm thick slices in axial reformation, 268 × 174 matrix size, 25° flip angle, 4.3-ms repetition time, 1.2-ms echo time, TFE factor 89, SENSE factor 1.4.

MRI was performed at different time-points: arrival of the contrast bolus was tracked and acquisition of the post-contrast dynamic phases were acquired after contrast agent was detected in the pulmonary arteries: arterial phase was started after 10 s, portal venous phase after 40 s and venous phase after 75 s. If the patient was not able to follow the breath-hold commands, the aforementioned times were adjusted slightly. Acquisition of subsequent dynamic MR images was continued for 30 min at intervals of 1 min. Each volume was imaged in a single breath-hold (mean imaging time per volume: 19 s). To ensure reproducibility of breath-hold position, data were acquired after expiration, and patients were instructed prior to the study to try and hold his or her breath at the same depth during each acquisition.

Post-processing

Post-processing was performed using in-house software written in Matlab (MATLAB and Statistics Toolbox Release 2013b, The MathWorks). Concentrations were calculated as the relative signal enhancement $S(t)/S_0 - 1$, where $S(t)$ is the post-contrast and S_0 the pre-contrast signal intensity [15, 16]. The haematocrit was determined beforehand in a blood sample and used to convert arterial and venous blood concentrations into plasma concentrations. The arterial and portal venous input regions of interest (freehand ROIs) were defined by an experienced radiologist inside the lumen of the abdominal aorta in the arterial phase and the portal vein in the portal venous phase, respectively, and selected pixel values were averaged to produce the arterial and portal venous input functions $C_a(t)$ and $C_p(t)$ (Fig. 2).

Similarly, one ROI was defined for each liver segment to arrive at the respective hepatic tissue concentration, C_L. Care was taken to exclude any visible vessels from the circular ROI, which was set to a diameter of 10 mm. The regions were visually controlled for inconsistencies due to breathing-related movement and corrected if necessary: First, signal concentration

Fig. 2 Acquired DCE MR images before contrast injection (A) and in the arterial (B), venous (C) and late (D) phases. The drawn regions of interest (ROIs) to determine relative signal enhancement comprise the abdominal aorta (red), the portal vein (blue) and a typical liver region (green)
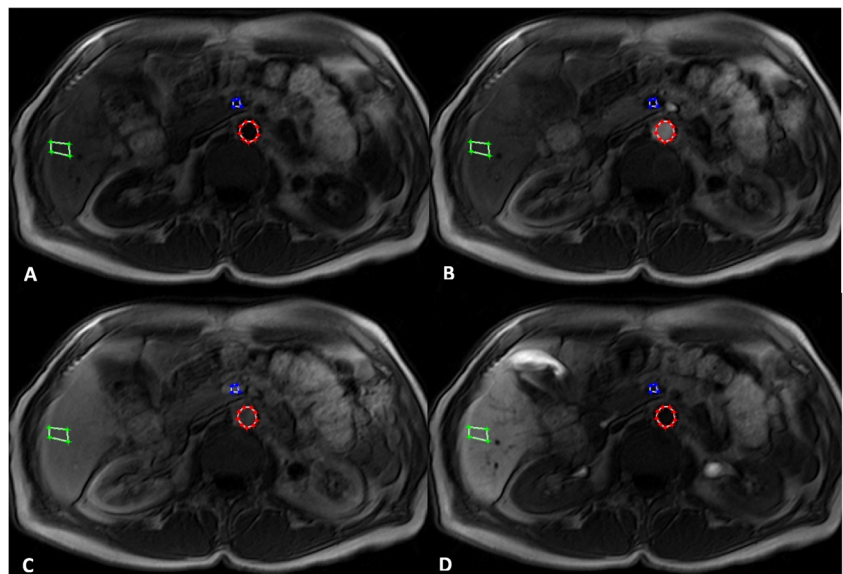
in the aorta and portal vein were assumed to take on the same value after intravascular equilibration of contrast medium concentration. If this was not the case, the chosen ROIs were checked again and corrected. Second, sudden and inconsistent changes of signal intensity where continuous behaviour could be expected were deemed suspicious of being outliers due to artefacts (e.g. breathing during image acquisition) and checked again. If an outlier was indeed found to be due to an artefact, the value was manually edited to be the average of the two adjacent – as in a timely manner – signal intensities.

Data analysis

Tissue parameters were determined by numerical simulation of C_L with different tissue parameters (AFF, V_i, K_u, K_e) given the measured values of C_a and C_p. For this, an optimisation procedure provided by the optimisation toolbox in Matlab was employed with fixed initial values.

To verify whether the hepatic excretion rate K_e is a necessary parameter in modelling the data, the optimisation procedures were repeated with K_e set to zero, effectively neglecting excretion in accordance with previous approaches by other groups. Henceforth the model with account for both excretion and uptake is referred to as the 'full' model, whereas the model with K_e held fixed at zero will be denoted as the 'conventional' model.

Finally, some of the previously published approaches utilised a standard five-phase imaging protocol to extract parameters of liver function [16]. To compare these approaches with the proposed extended acquisition, the optimisation procedures were repeated for both the conventional and full

model and only the first five data points were taken into account – here this is referred to as 'reduced data'.

Results

Dynamic signal intensities over a time-span of 30 min were successfully acquired in 16 patients. Two patients were excluded from the subsequent analysis due to the presence of severe breathing-related artefacts, which prohibited a reliable determination of the portal venous signal intensity. Aortic and hepatic signal intensities could be reliably detected in all 16 patients. The mean fat fraction over all 16 patients was 5.9 ± 3.4 % (range: 1.8–8.7).

A typical time-intensity curve of liver parenchyma together with the aortic and portal venous signal enhancement is shown in Fig. 3. Figure 4 demonstrates the mean time course of relative signal enhancement over all patients and the respective variation as denoted by the standard deviation. Enhancement of intact hepatic tissue was deemed homogeneous in all patients by qualitative visual assessment.

The mean-squared distance between measured and simulated results over all patients and liver segments in units of relative signal enhancement was significantly higher ($p<0.05$) for the conventional model ($9.2*10^{-2} \pm 2.8*10^{-2}$) than for the full model ($0.8*10^{-2} \pm 0.2*10^{-2}$). The agreement between measured and simulated hepatic signal enhancement is demonstrated in Fig. 5a and b. The mean uptake rate over all patients and liver segments for the full model was $K_{u,\,full}=4.02 \pm 1.32$ /100/min, while the uptake rate for the conventional

Fig. 3 Relative signal enhancement for aorta, portal vein and a typical liver region (male patient, 62 years, region of interest (ROI) set in liver segment IV). Note that relative signal enhancement is similar for both the aorta and portal vein for times greater than 10 min as can be expected due to equilibration of gadoxetic acid in the vascular space
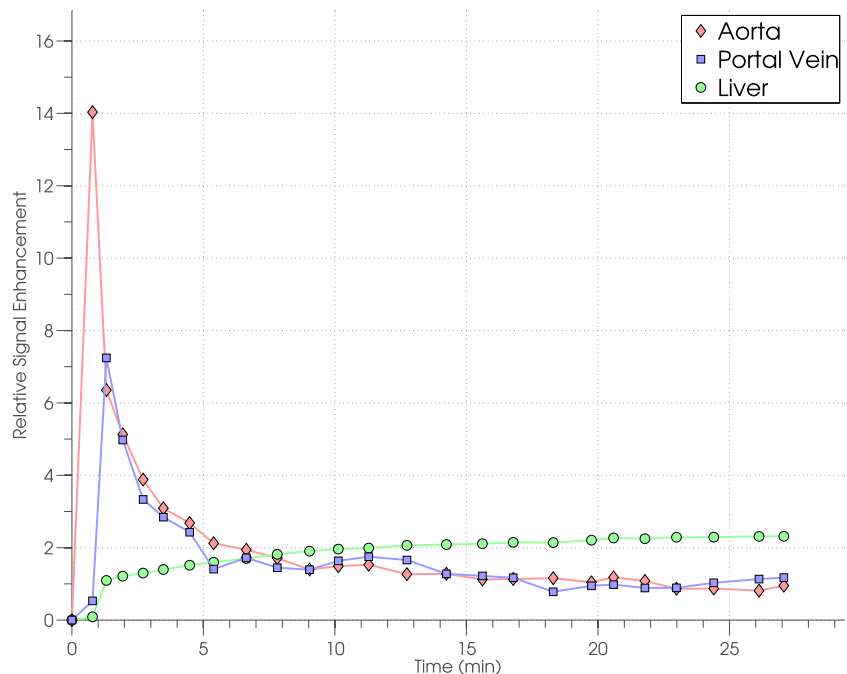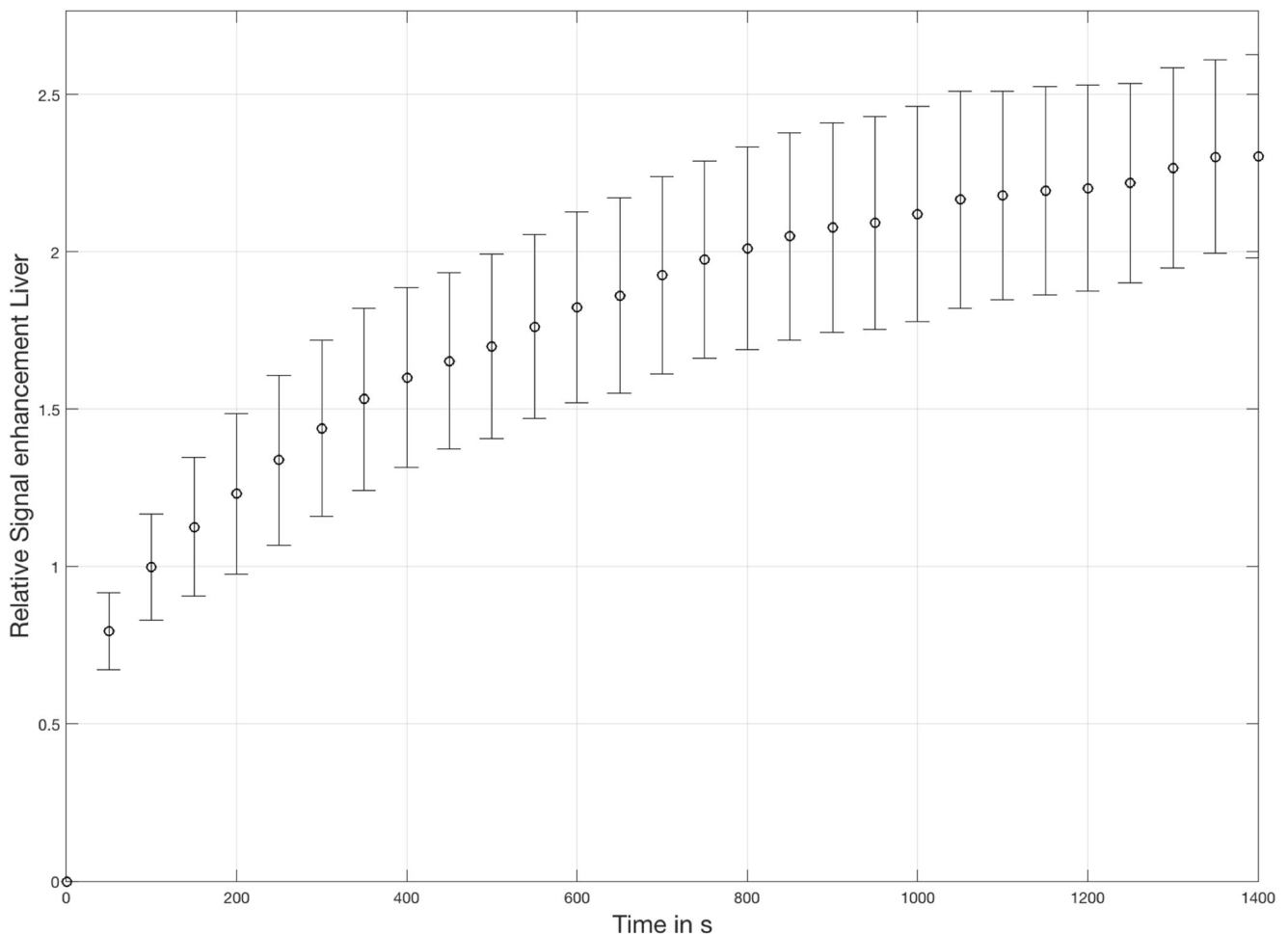
Fig. 4 Mean relative signal enhancement in the liver and corresponding standard deviation over all patients. As times of measurements were slightly different for each patient a linear interpolation was used to arrive at measurements at standardised times of n*50s for n=28 for each patient

model was both lower and had a wider range with $K_{u, conv}$=3.78 ± 1.96 /100/min.

The mean extracellular volume fractions for the full and conventional model were comparable with $V_{e,full}$= 0.20 ± 0.08 and $V_{e,conv}$=0.22 ± 0.12. Similarly, the extracted values for the arterial flow fraction were comparable although slightly higher for the conventional model, with AFF_{full}= 0.08 ± 0.04 and AFF_{conv}=0.11 ± 0.06. The full model allowed the calculation of an effective excretion half-time as a measure of the hepatic excretion of gadoxetic acid, which was found to be 23.3+/-6.8 minutes over all liver segments and patients.

Intraindividual variation of the excretion half-time between liver segments was found to be lower with a standard deviation of 3.2 min than interindividual variation with a standard deviation of 6.8 min.

Results of applying the full and conventional model to the first five data points exclusively are shown in Fig. 5c and d. Mean squared distances between measured and simulated results were $1.2*10^{-4} ± 0.7*10^{-4}$ and $3.6*10^{-4} ± 2.3*10^{-4}$, respectively. The mean values and standard deviation of all extracted parameters of the models are summarised in Tables 1

and 2, which give the overall mean values and detailed mean values for each liver segment.

Discussion

In this work, we have demonstrated that the proposed model that accounts for both uptake and excretion of gadoxetic acid is capable of accurately replicating the measured amount of hepatic gadoxetic acid based on an augmented routine clinical protocol. The time curve of hepatic signal intensities over a course of 30 min after administration of gadoxetic acid is thus condensed into a set of four tissue parameters that may be tested for clinical utility in future studies.

The ever-increasing demand of quantitative measures of liver function [5–10, 12, 13] explains the rising interest in non-invasive means of quantifying liver perfusion and contrast uptake locally [15, 16, 19, 20]. Especially the existence of diffuse or focal liver disease might render an assessment of local liver function more appealing than existing measures of its global function as liver function reserve estimation is
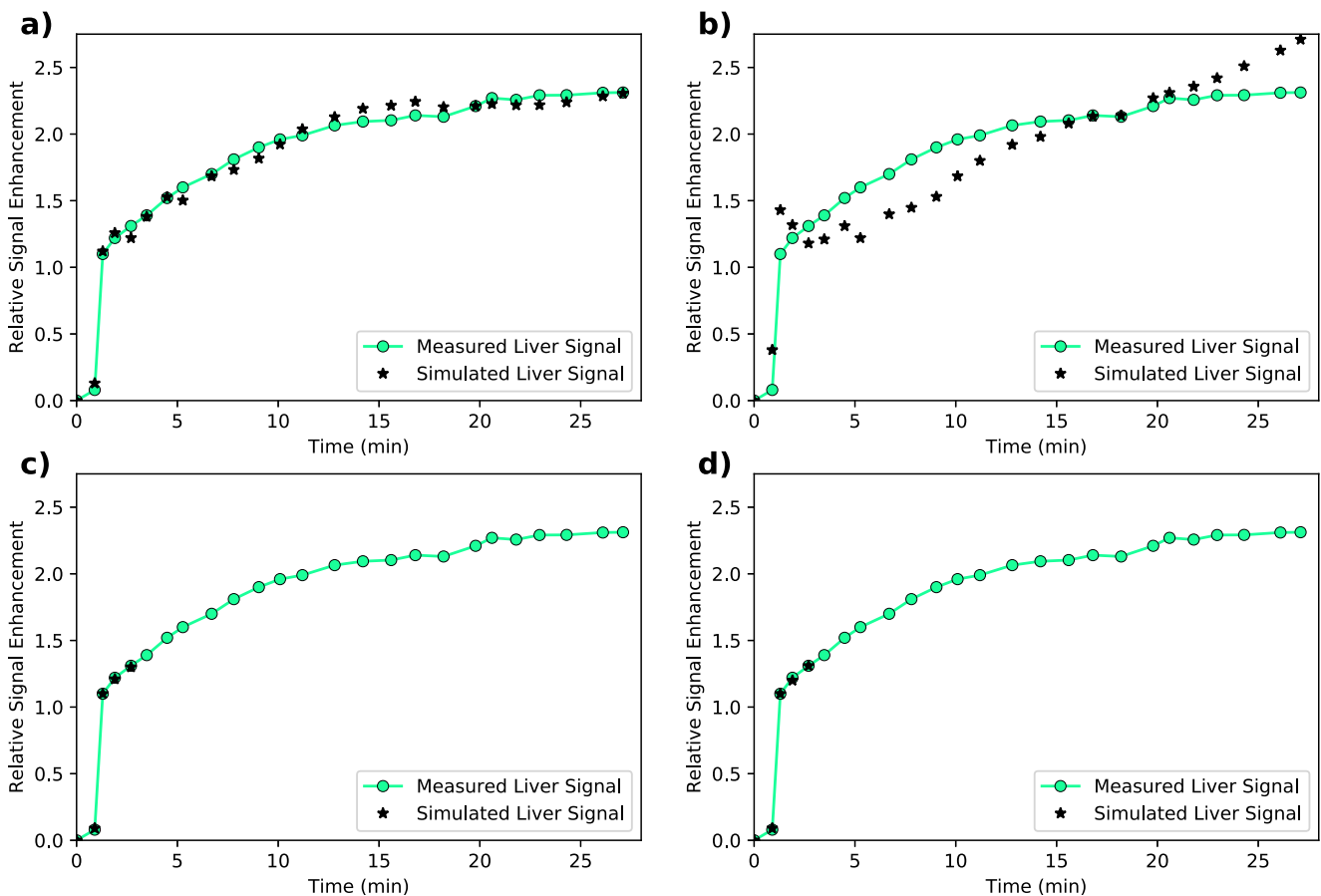
Fig. 5 Measured and simulated relative signal enhancement for the complete four-parameter dual-inlet two-compartment uptake and excretion model (**a**). A good agreement between modelled and measured signal enhancement values in a typical liver region can be seen. Note that the deviation between measured and simulated values is much lower than for the conventional model, which shows a clear disagreement (**b**). When only the first five measurements are taken into account, both the novel model with excretion (**c**) and the conventional model (**d**) demonstrate a good agreement between measured and simulated relative signal enhancement

important for selecting appropriate patients for hepatectomy or ablation of tumours [21]. The model presented in this work allows for a local estimation of liver function, which might even be assessed on a voxelwise level if necessary in case of diffuse or focal liver disease. Many previously published models for liver function did not apply compartment models that consider the quantitative measures of hepatic gadoxetic excretion [1, 5, 7, 10, 14–16, 19, 22, 23]. Although it was

shown that measures of hepatic uptake can provide a suitable method for the evaluation of liver functional reserve [24] and to quantitatively estimate liver function [20], models of liver function can be further improved, as hepatic gadolinium amount is influenced by both uptake and excretion simultaneously. Our model takes the aortic and portal venous signal enhancement as inputs and models the liver enhancement based on both the uptake of gadoxetic acid from plasma into

Table 1 Extracted model parameters for both the full and the conventional model when applying them to the full amount of available data (measured over a time span of 30 min) and when applying them to a reduced amount of data (first five acquired DCE MR images, time span ca. 3 min)

	K_u (/100/min)	V_e	AFF	$T_{1/2,e}$ in min
Full model – full data	4.02 ± 1.32	0.20 ± 0.08	0.08 ± 0.04	23.3 ± 6.8
Conventional model – reduced data	4.93 ± 1.74	0.21 ± 0.12	0.08 ± 0.05	N/A
Full model – reduced data	5.82 ± 1.59	0.18 ± 0.09	0.07 ± 0.05	24.5 ± 12.4
Conventional model – full data	3.78 ± 1.96	0.22 ± 0.12	0.11 ± 0.06	N/A

Table 2 Extracted model parameters for the full model for different liver segments with their respective standard deviations

Liver segment	I	II	III	IVa	IVb	V	VI	VII	VIII
K_u (/100/min)	4.14 ± 1.42	3.93 ± 1.34	3.82 ± 1.45	3.51 ± 1.08	3.90 ± 1.47	4.44 ± 1.10	4.01 ± 1.29	3.71 ± 1.31	4.70 ± 1.15
V_e	0.20 ± 0.09	0.18 ± 0.07	0.22 ± 0.10	0.18 ± 0.09	0.17 ± 0.09	0.21 ± 0.07	0.17 ± 0.11	0.17 ± 0.07	0.28 ± 0.12
AFF	0.07 ± 0.05	0.09 ± 0.06	0.05 ± 0.04	0.10 ± 0.06	0.08 ± 0.06	0.08 ± 0.05	0.08 ± 0.04	0.07 ± 0.05	0.12 ± 0.07
$T_{1/2,e}$ in min	24.0 ± 5.1	23.7 ± 5.3	21.3 ± 4.2	25.3 ± 5.5	24.5 ± 6.1	21.4 ± 4.9	25.0 ± 5.7	23.4 ± 5.3	21.5 ± 6.5

hepatocytes as well as its excretion from hepatocytes into bile ducts. Accordingly, a parameter (K_e) was added to the model to account for the biliary clearance of gadoxetic. Whereas hepatic uptake of gadoxetic acid occurs comparatively quickly, with most of the contrast medium that ultimately is transported to the hepatocytes being taken up during the first 5 min after contrast agent administration, its biliary excretion is a much slower process that requires longer observation times. Accordingly, we measured hepatic enhancement kinetics for a prolonged period of time, i.e. 30 min. Doing so permits not only the extraction of an additional quantitative parameter (excretion rate K_e), but also improves the precision with which we can model hepatic gadoxetic kinetics. Recently, a study published by Georgiou et al. [11] considered hepatic excretion in ten healthy volunteers with a model considering five parameters. This requires a more densely sampled time curve to arrive at a sufficient number of measurements in order to avoid overfitting and may require compromises in terms of spatial resolution or signal to noise ratio. Furthermore, no comparison to established models that consider uptake only was made. As demonstrated by Fig. 5a, the proposed approach precisely models hepatic signal enhancement over the complete observed time course. Including gadoxetic acid excretion into the model is indeed necessary: without it, an infinite accumulation of intracellular hepatic gadoxetic is modelled mathematically – thus preventing a good agreement between modelled and measured liver signal enhancement (see Fig. 5b). Consequently, the extracted parameters showed the least variation when applying the full dual-inlet two-compartment model that accounts for excretion (Table 1). This indicates that the proposed model extracts liver functional parameters more precisely than previously employed methods that consider uptake only. Saito et al. used a standard five-phase imaging protocol to measure hepatic uptake without taking into account hepatic excretion [16]. This corresponds to the situation of applying the conventional model to the reduced data, and thus leads to less precise results, as demonstrated by the higher standard deviation. Quantitative uptake rates derived from our model are in good agreement with previously published experiments: K_u was determined as 4.02 ± 1.32 /100/min

in our study, compared with 3.4 ± 1.9 /100/min in normal-appearing liver tissue by Sourbron et al., or a range from 0.79 to 7.81 /100/min by Saito et al. [15, 16]. Our model allows the determination of the parameter 'excretion half-time' ($T_{1/2,e}$). This parameter yielded consistent results across the liver parenchyma of a given patient, i.e. exhibited only a small variation between liver segments in the same patient; as one would expect, variations were greater across different patients. This finding was also corroborated by the visual assessment of the liver, which exhibits homogeneous enhancement in all 16 patients. There is increasing evidence to suggest that a quantitation of liver gadoxetic acid excretion per se is at least as important a parameter as is gadoxetic acid uptake ± quite likely in view of the dual function of the liver. Excretion of hepatocyte-specific contrast medium through the bile duct has been found to correlate well with the severity of primary sclerosing cholangitis [12] and is associated with an increased risk for 1-year mortality after liver transplantation [13]. However, in these studies hepatic excretion was only qualitatively assessed by the presence of contrast medium in the bile ducts. The model proposed in this work might enable further examination of these correlations by providing quantitative and accurate measures for both uptake and excretion values. Translation into clinical practice will be facilitated by the fact that the method described here is fully compatible with standard pulse sequence protocols for dynamic contrast-enhanced liver MRI: it builds upon the standard 4-phase imaging protocol used clinically for detection and characterisation of focal and diffuse liver lesions. Accordingly, liver function can be assessed as an 'add-on', without interfering with the acquisition of the usual diagnostic pulse sequences needed in patients undergoing liver MRI.

By doing so, however, we had to compromise on temporal resolution. With the usual four-phase dynamic acquisition (i.e. pre-contrast, arterial, portal-venous, and venous phase), temporal resolution is limited, which limits the validity with which AFF can be determined. To solve this problem, a fixed value for the AFF was proposed [16], although information about the true nature of the AFF is lost that way. Increasing the temporal resolution would be another option [15], and our model could be applied to such data as well; however,

increasing the temporal resolution is usually only achievable at the expense of spatial resolution, which would not be acceptable for most clinical hepatic MRI pulse sequence protocols. As demonstrated in Fig. 3, the most rapid dynamic changes occur within the first 5 min. The DCE signal might be sampled continuously for the first 5 min with high temporal resolution, followed by an interleaved acquisition of other diagnostic pulse sequences, such as T2-weighted imaging. A second set of low temporal resolution DCE sequences could be acquired and the missing data at the intermediate time points might be amenable to interpolation. However, in that case, care would have to be taken to keep internal scanner parameters, most prominently receiver gain, at fixed levels.

Our study has limitations: First, concentrations were calculated based on the relative signal enhancement $S(t)/S_0 - 1$ [15, 16]. More accurate concentration measurements could be based upon T1 relaxometry. However, this would mean another prolongation of acquisition times, and/or requires one to compromise on spatial or temporal resolution. Parallel imaging was used to shorten the acquisition time. Although no artefacts were visible with the chosen SENSE factor of 1.4, subtle signal alterations due to patient movement or small coil displacements are possible and might influence model parameters. However, this limitation was accepted in light of the above-mentioned trade-off between spatial and temporal resolution. An additional limitation is that gadoxetic acid relaxivity in the intracellular milieu may differ from relaxivity in plasma [25]. Another limitation is the fact that most of the patients had already undergone possible hepato-toxic systemic chemotherapy, such that our patient volunteers may not be representative for a completely normal liver function. Last, further studies are needed to investigate the utility of our model in patients with liver damage, and patients with restrictions in hepatobiliary excretion. Validation of the results could be based upon the MELD score as used by Haimerl et al. [1] and on specific tests of global liver function such as the recently introduced LiMAx test [26] or existing conventional liver function tests like Tc-99 GSA or indocyanine green retention. It should be noted that it is beneficial to take liver volume into account when comparing local measures of liver function – such as presented in this work – with tests of global liver function as demonstrated recently [27].

The proposed model gives an accurate representation of the observed signal intensity values and transfers them into a set of four tissue parameters that can be locally evaluated, thus providing a means to estimate local liver function. In addition to widely established models, an excretion parameter is provided that helps in gaining a more accurate radiological surrogate of liver function. Based upon this work, further research in dedicated clinical settings will show if the promise of clinical utility of these parameters can be upheld.

Compliance with ethical standards

Guarantor The scientific guarantor of this publication is Prof. Christiane Kuhl.

Conflict of interest The authors of this manuscript declare no relationships with any companies whose products or services may be related to the subject matter of the article.

Statistics and biometry No complex statistical methods were necessary for this paper.

Informed consent Written informed consent was obtained from all subjects (patients) in this study.

Ethical approval Institutional Review Board approval was obtained.

Methodology
• prospective
• experimental
• performed at one institution

References

1. Haimerl M, Verloh N, Fellner C et al (2014) MRI-based estimation of liver function: Gd-EOB-DTPA-enhanced T1 relaxometry of 3T vs. the MELD score. Sci Rep 4:5621
2. Ryeom HK, Kim SH, Kim JY et al (2004) Quantitative evaluation of liver function with MRI Using Gd-EOB-DTPA. Korean J Radiol 5:231–239
3. Kim T, Murakami T, Hasuike Y et al (1997) Experimental hepatic dysfunction: evaluation by MRI with Gd-EOB-DTPA. J Magn Reson Imaging 7:683–688
4. Tsuda N, Harada K, Matsui O (2011) Effect of change in transporter expression on gadolinium-ethoxybenzyl-diethylenetriamine pentaacetic acid-enhanced magnetic resonance imaging during hepatocarcinogenesis in rats. J Gastroenterol Hepatol 26:568–576
5. Bastati N, Feier D, Wibmer A et al (2014) Noninvasive differentiation of simple steatosis and steatohepatitis by using gadoxetic acid-enhanced MR imaging in patients with nonalcoholic fatty liver disease: a proof-of-concept study. Radiology 271:739–747
6. Haimerl M, Verloh N, Zeman F et al (2013) Assessment of clinical signs of liver cirrhosis using T1 mapping on Gd-EOB-DTPA-enhanced 3T MRI. PLoS One 8:e85658
7. Noren B, Forsgren MF, Dahlqvist Leinhard O et al (2013) Separation of advanced from mild hepatic fibrosis by quantification of the hepatobiliary uptake of Gd-EOB-DTPA. Eur Radiol 23:174–181
8. Verloh N, Haimerl M, Rennert J et al (2013) Impact of liver cirrhosis on liver enhancement at Gd-EOB-DTPA enhanced MRI at 3 Tesla. Eur J Radiol 82:1710–1715
9. Nilsson H, Blomqvist L, Douglas L, Nordell A, Jonas E (2010) Assessment of liver function in primary biliary cirrhosis using Gd-EOB-DTPA-enhanced liver MRI. HPB (Oxford) 12:567–576

10. Verloh N, Haimerl M, Zeman F et al (2014) Assessing liver function by liver enhancement during the hepatobiliary phase with Gd-EOB-DTPA-enhanced MRI at 3 Tesla. Eur Radiol 24:1013–1019

11. Georgiou L, Penny J, Nicholls G et al (2017) Quantitative Assessment of Liver Function Using Gadoxetate-Enhanced Magnetic Resonance Imaging: Monitoring Transporter-Mediated Processes in Healthy Volunteers. Invest Radiol 52:111–119

12. Ringe KI, Hinrichs J, Merkle EM, Weismuller TJ, Wacker F, Meyer BC (2014) Gadoxetate disodium in patients with primary sclerosing cholangitis: An analysis of hepatobiliary contrast excretion. J Magn Reson Imaging 40:106–112

13. Wibmer A, Aliya Q, Steininger R et al (2012) Liver transplantation: impaired biliary excretion of gadoxate is associated with an inferior 1-year retransplantation-free survival. Invest Radiol 47:353–358

14. Wibmer A, Prusa AM, Nolz R, Gruenberger T, Schindl M, Ba-Ssalamah A (2013) Liver failure after major liver resection: risk assessment by using preoperative Gadoxetic acid-enhanced 3-T MR imaging. Radiology 269:777–786

15. Sourbron S, Sommer WH, Reiser MF, Zech CJ (2012) Combined quantification of liver perfusion and function with dynamic gadoxetic acid-enhanced MR imaging. Radiology 263:874–883

16. Saito K, Ledsam J, Sourbron S et al (2013) Assessing liver function using dynamic Gd-EOB-DTPA-enhanced MRI with a standard 5-phase imaging protocol. J Magn Reson Imaging 37:1109–1114

17. Sharma A, Houshyar R, Bhosale P, Choi JI, Gulati R, Lall C (2014) Chemotherapy induced liver abnormalities: an imaging perspective. Clin Mol Hepatol 20:317–326

18. Kim H, Taksali SE, Dufour S et al (2008) Comparative MR study of hepatic fat quantification using single-voxel proton spectroscopy, two-point dixon and three-point IDEAL. Magn Reson Med 59:521–527

19. Geisel D, Ludemann L, Keuchel T et al (2013) Increase in left liver lobe function after preoperative right portal vein embolisation assessed with gadolinium-EOB-DTPA MRI. Eur Radiol 23:2555–2560

20. Yoon JH, Lee JM, Paek M, Han JK, Choi BI (2016) Quantitative assessment of hepatic function: modified look-locker inversion recovery (MOLLI) sequence for T1 mapping on Gd-EOB-DTPA-enhanced liver MR imaging. Eur Radiol 26:1775–1782

21. Manizate F, Hiotis SP, Labow D, Roayaie S, Schwartz M (2010) Liver functional reserve estimation: state of the art and relevance to local treatments. Oncology 78(Suppl 1):131–134

22. Dahlqvist Leinhard O, Dahlstrom N, Kihlberg J et al (2012) Quantifying differences in hepatic uptake of the liver specific contrast agents Gd-EOB-DTPA and Gd-BOPTA: a pilot study. Eur Radiol 22:642–653

23. Choi JW, Lee JM, Kim SJ et al (2013) Hepatocellular carcinoma: imaging patterns on gadoxetic acid-enhanced MR Images and their value as an imaging biomarker. Radiology 267:776–786

24. Saito K, Ledsam J, Sourbron S et al (2014) Measuring hepatic functional reserve using low temporal resolution Gd-EOB-DTPA dynamic contrast-enhanced MRI: a preliminary study comparing galactosyl human serum albumin scintigraphy with indocyanine green retention. Eur Radiol 24:112–119

25. Rohrer M, Bauer H, Mintorovitch J, Requardt M, Weinmann HJ (2005) Comparison of magnetic properties of MRI contrast media solutions at different magnetic field strengths. Invest Radiol 40:715–724

26. Stockmann M, Lock JF, Malinowski M, Niehues SM, Seehofer D, Neuhaus P (2010) The LiMAx test: a new liver function test for predicting postoperative outcome in liver surgery. HPB (Oxford) 12:139–146

27. Haimerl M, Schlabeck M, Verloh N et al (2016) Volume-assisted estimation of liver function based on Gd-EOB-DTPA-enhanced MR relaxometry. Eur Radiol 26:1125–1133